EFFECTS OF LARGE-SCALE TURBULENCE ON CYCLIC VARIABILITY IN SPARK-IGNITION ENGINE

A. A. Burluka*, A.M.T.A. El-Dein Hussin*,, Z.-Y. Ling* and C.G.W.Sheppard***
A.A.Burluka@leeds.ac.uk
*School of Mechanical Engineering, The University of Leeds,
Leeds, West Yorkshire, LS25 3AN, The United Kingdom
**Permanent address: Department of Mechanical Power Engineering,
Ain Shams University, Cairo, Egypt

Abstract
An investigation is carried out into the connection between the various characteristics of the velocity field and the burning rate in a spark-ignition engine. The experiments are performed on the Leeds University Ported Optical Engine with a large skip-firing ratio; the engine allows a full optical access to the combustion chamber. Velocity fields are obtained using a PIV and a systematic distinct averaging is performed with an account of the cyclic variability of the burning rate, that is the properties of the turbulent velocity fields are derived separately for the fast, middle and slow cycles using the peak pressure as a proxy measure for the burning rate. Even though the velocity fields are nearly homogeneous in the mean they reveal very significant intermittency where the regions of intense fluctuations have an extent more than half the clearance height. It is shown that the variations of the burning rate are correlated with the fluctuations in root-mean-square fields of the velocity magnitude, vorticity and shear strain rate. Faster combustion is induced by the fields with larger rms. No discernible correlation of the burning rate with the average vorticity or shear strain fields has been detected. The integral scales of the large-scale motion derived from the PIV do not show any systematic variation between fast and slow cycles.

Introduction
Cycle-to-cycle variability (ccv) is caused by variations in instantaneous combustion rates between different cycles while the engine operates at nominally identical operating conditions. These variations are an impediment to improving the performance of an engine [1]. This is caused by the fact that under operating conditions at the knock boundary, the octane number requirements, maximum compression ratio and spark timing are all limited by the propensity for autoignition to occur in the fastest burning cycles [1, 2, 3]. Furthermore, the spark timing for a given running condition is typically optimised for the heat release profile of the most frequent cycle, hence any deviation from this optimum will entrain penalties in terms of lost power and efficiency. Strong ccv, such that the variation in IMEP is greater than 10%, is noticeable to the driver as a deterioration in the vehicle driveability [1]. The review [4] suggests that total elimination of cycle-to-cycle variation would result in a 10% increase in brake power output for the same fuel consumption. Unfortunately, the current trend in engine design favours an increase of the amount of exhaust gas recirculation which, together with lean combustion, lead to increased cyclic variability. In particular, cycle-to-cycle variation in early flame development restricts lean operation for any particular fuel [5].

There is a number of potential sources of ccv [1, 3, 6], among which are the variability in: a) charge motion and "turbulence" during combustion; b) the trapped amounts of fuel, air, and residual and/or recirculated exhaust c) uniformity of the mixture composition within the cylinder, especially near the spark plug, associated with imperfect mixing between the air, fuel and residual or recirculated exhaust; d) spark discharge characteristics, such as breakdown energy and initial flame kernel random displacement. Some of the above-mentioned factors are of much greater importance than others [6]. An attempt to describe ccv in the framework of the

thermodynamic modelling has been made in [6] and it has been found that imposing a 10% variation in the rms velocity at the moment of ignition allows quite a good estimation of ccv of peak pressure. Variation of the equivalence ratio of the charge has been identified as the second main cause of ccv producing a spread of values of the maximum pressure occurring at the same crank angle. At the same time, the variation of the rms velocity between the individual cycles was introduced in [6] in an ad-hoc manner, in particular, no experimental evidence has so far been available to support this work. The main purpose of this work is to explore the extent of the large-scale flow variability from one cycle to another and to establish what are the main flow characteristics affecting the burning rate in an individual cycle.

While the present measurements are performed in an engine, it should be stressed that fluctuations of burning rate are common for every instance of turbulent premixed flames. ~In that sense, the flame propagation in an engine is not different from explosions in closed volumes or freely propagating flames. Indeed, as early as 1953 Mickelsen and Ernstein [7] in their pioneering work observed that the burning rate of a free turbulent flame in a wind tunnel was a random quantity, the distribution of which was approximately Gaussian. For stronger turbulence and for non-stoichiometric mixtures the variance of burning rate was found to increase. The variations in burning rates observed by Mickelsen and Ernstein [7] must be attributed entirely to the variation of the flow filed, because the effect of variation in the spark discharge properties and other parameters were ruled out through a carefully executed experimental arrangement. It was found that there was very little correlation between either the spark current, spark energy or spark kernel displacement and the observed turbulent flaame speed [7]. Large variations in burning rate have been observed for very diverse fuels and conditions in turbulent deflagrations in fan-stirred bombs, where the charge composition is perfectly uniform and well controlled [8, 9].

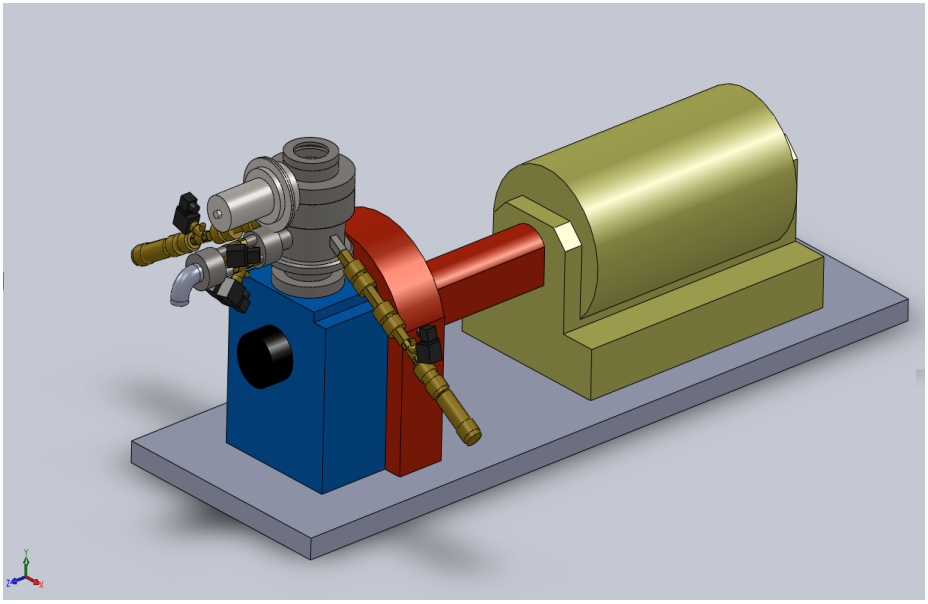

Figure 1. Arrangement of the single cylinder LUPOE2 engine showing the intake and exhaust systems, a decompression valve, and the dynamometer.

Shen et al. [10] performed simulations of an SI engine using different sub-models to simulate variability in flaame kernel convection, level of turbulence experienced by the flaame kernel during the early stages of combustion and the level of turbulence experienced during the main flaame propagation.on.n... They suggested that ccv in turbulence, particularly during the early stages of combustion, had the largest impact. The predominance of the fluuid flow factor (more specifically, variations in the turbulence conditions experienced by the developing flaame kernel) on ccv in freely propagating explosions has been demonstrated by Lipatnikov

and Chomiak [11].1].]... This work established the link between the internal intermittency of turbulence, which is manifested in the log-normal distribution for the instantaneous values of the dissipation, and the amplitude of the spread in the turbulent diffusivity defining the flame growth.

Experimental equipment

The experiments have been performed on a single cylinder bespoke Leeds University Ported Optical Engine, Make 2, or LUPOE2 [3, 12]. The characteristic feature of LUPOE2 is that the common in other engines overhead valves are replaced by ports so as not to obstruct the optical access. A disc-shaped head was used in this work; in it were fitted top quartz window of the same diameter as the engine bore and two side quartz windows in order to provide a full optical access.

LUPOE2 has two diametrically opposed intake ports of rectangular cross section and an exhaust passage consisting of a collander, four rings of of circular exhaust holes drilled in the liner, communicating with a void between a liner and barrel leading to one exhaust duct, see Fig. 1. The time of ports opening and closure are controlled by the movement of piston. The fuel, ETBE10 representative of the modern blend with 10% of the bio-derived oxygenated compounds, is introduced into the heated intake duct well upstream of the port through a needle; both air and fuel flowrates are metered in required proportions to an accuracy of 2% in the average, each of the two intakes has its own flowmeters. The purpose of this ported breathing arrangement is to eliminate swirl and tumble motion often existing in valved engines, and to generate as uniform in-cylinder flow field as possible. In this work, a central spark ignition was employed and most of the results shown below were obtained with a spark advance of -17 deg. BTDC.

Table 1. LUPOE2 specifications

Parameter	
Bore [m]	0.08
Stroke [m]	0.11
Conrod length [m]	0.232
Crank radius, [m]	0.055
Inlet port opening/closure, [deg. CA]	-116
Exhaust port opening/closure, [deg. CA]	115.5
Compression ratio, [-]	11.5
Volume of top land crevice, [mm^3]	1450
Spark advance, [deg. CA]	-17

Control of trapped residuals in ported engines is difficult; to gain a control of mixture composition, the LUPOE2 has a bespoke decompression valve allowing to skip the firing of a number of consecutive cycles. It can be seen on the top left of the barrel in Fig. 1. It has been found that a skip-firing ratio, i.e. number of skipped cycles, of five eliminates both the trapped and recirculated residuals. The present results were obtained with the skip-firing ratio of 9. Other engine parameters are summarised in the Table 1; further details may be found in [12].

The combustion events in the engine were investigated using the schlieren photography with flame viewed from the top of the chamber and the pressure recording. The former method registers the flame leading edge while the mass fraction of the burnt charge may be derived from the latter. The intake flow was seeded with olive oil using SCITEC LS-10 seeding system, then the average and turbulent velocity field were measured using PIV system consisting of a double-pulsed Nd:Yag laser and a CCD-camera under control of LaVison DaVis software [13]. The PIV pixel-to-pixel resolution was 0.526 mm. Exhaustive description of the experimental set-up may be found in [12].

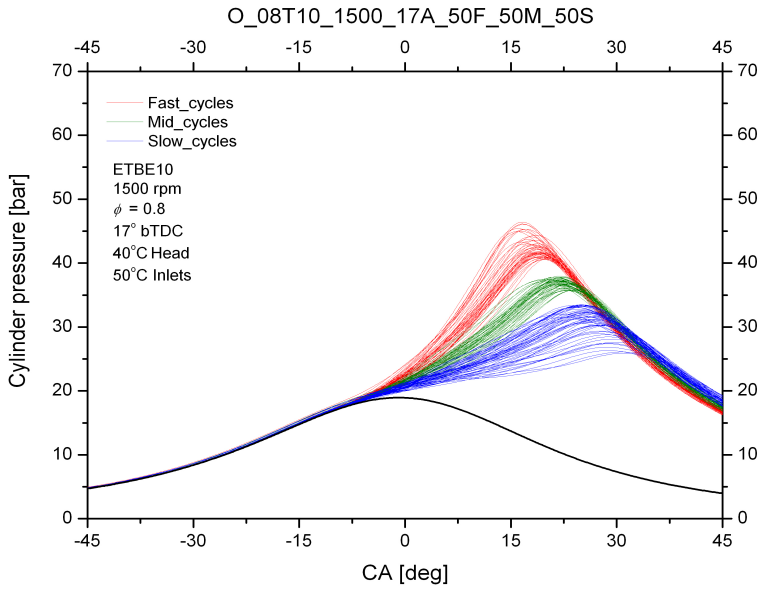

Figure 2. Spread of the crank-resolved pressure history of the firing cycles showing fifty samples of fast, middle and slow combustion events.

Cyclic variability of combustion

Figure 2 illustrates the spread of the crank-resolved pressure trace in firing cycles, illustrating a selection of fifty slow, middle and fast combustion events. The selection criterion adopted here is the peak pressure. The cycle is termed as “slow”, “middle” or “fast” if the peak pressure is below, within, or above the one standard deviation from the average value. While the peak pressure is not the only possible criterion for discerning the ccv, there exists fairly straightforward relationship between the peak pressure and other possible parameters, such as imep or the crank angle of the peak pressure; the adopted definition is illustrated in the Fig. 3 showing the relationship between the peak pressure and the crank angle at which it is achieved.

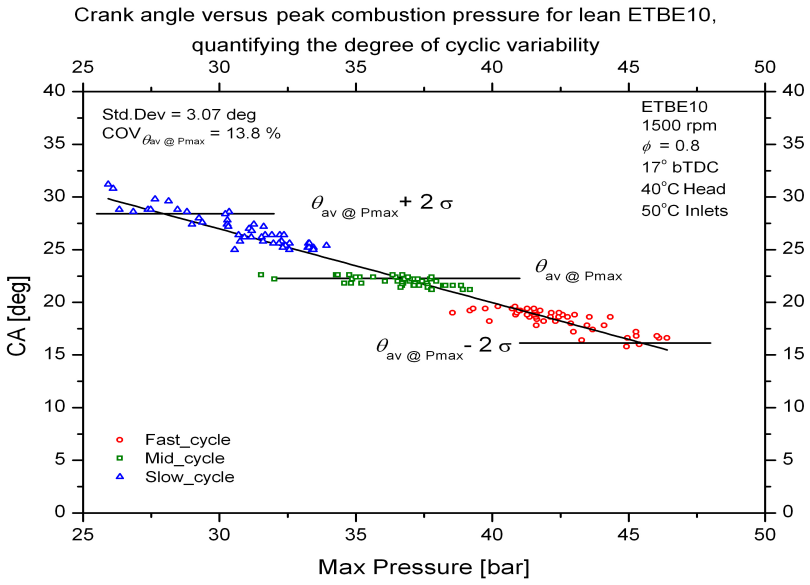

Figure 3. Relationship between the peak pressure and the crank angle at which it is achieved.

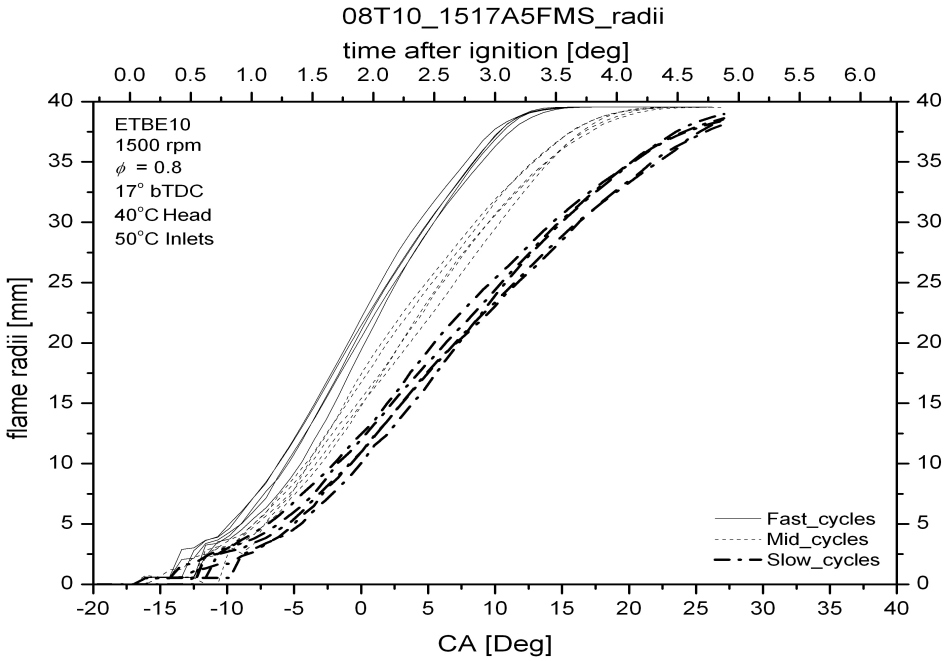

Figure 4. Cyclic variability in the flame leading edge propagation.

This variability is manifest also in the different rates of the flame growth, illustrated in Fig. 4 derived from the schlieren images. The flame radius is defined as the radius of a circle having the same area as the observed irregular flame contour.

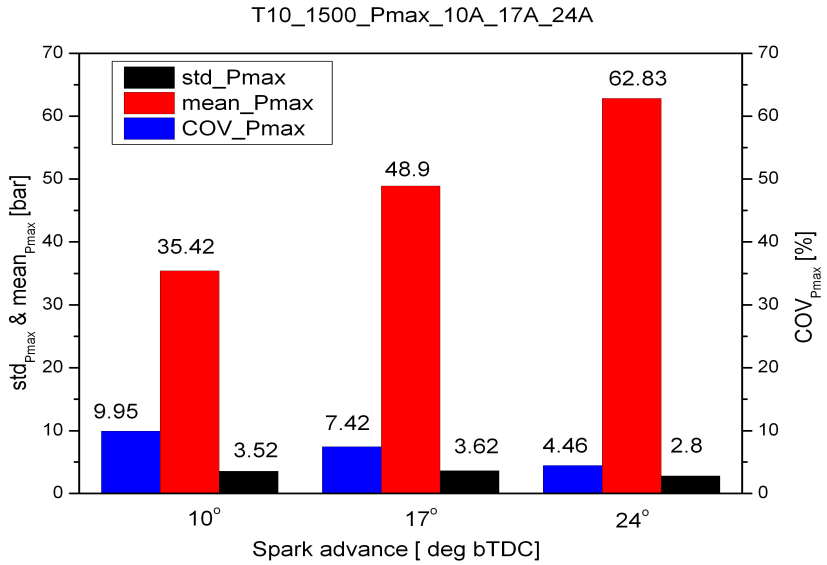

Figure 5. Influence of the spark advance on the magnitude of the cycle-to-cycle variations.

It may be inferred from Fig. 4 that there is a correlation between the burning rates for small and large flame kernels, and generally speaking, the cycles which start slow will remain slow. However, this correlation fails within a given group as some flames are slower when small but accelerate stronger and become faster at later stages of propagation, see the crossing lines in Fig. 4. Overall, the variability in the combustion duration, taken here as the time required for the flame to reach the size of 40mm, is approximately 20%, see Fig. 4. Nonetheless, the magnitude of ccv is related to the rate of combustion: for a fixed engine geometry and fuel composition different ignition timing will alter the burning rate. The results

obtained for three different ignition timings are shown in Fig. 5; one can see that higher peak pressures resulting from the spark advance at 24 deg. bTDC, indicative of faster burning, have also the lowest values of the standard variation in the peak pressure. This dependency is not monotonous as moving the timing from 10 deg. bTDC to 17 bTDC increases the burning rate but leaves the varability unchanged. In what follows, the emphasis is put on the fixed spark advance of -17^0 CA and the issues of the variability in the flame development dynamics shall not be pursued any further in this work.

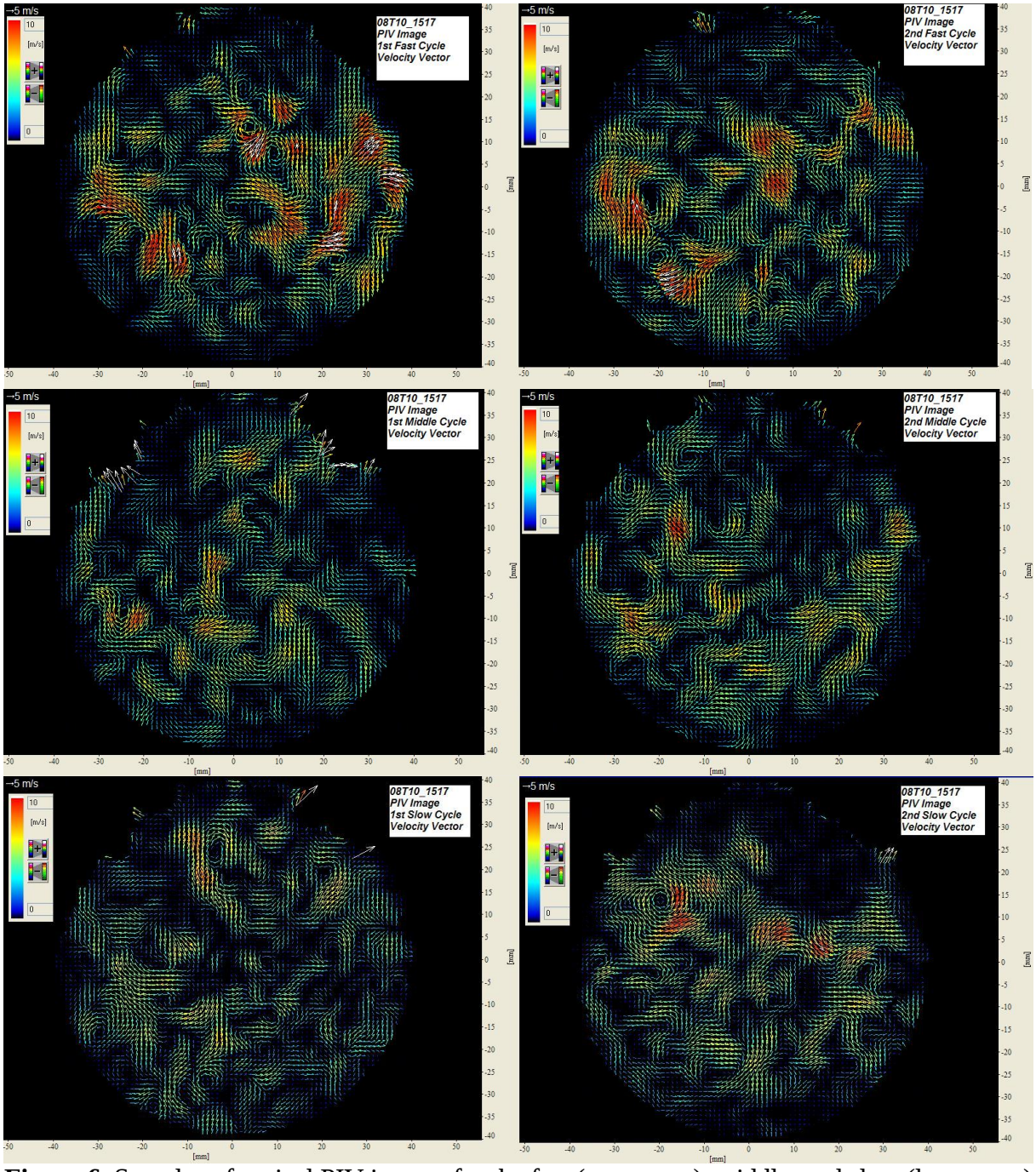

Figure 6. Samples of typical PIV images for the fast (upper two), middle, and slow (lower two) cycles. The colour bars show the magnitude of the velocity vectors

Cyclic variability of the flow field

Following a long-standing practice [1, 8, 14], an attempt is made here to correlate the combustion characteristics with the properties of the cold flow turbulence. For each cycle

shown in Fig. 1, a PIV snapshot was taken at the moment of ignition and variability of this images is studied below. Figure 6 shows typical PIV fields from fast, middle and slow cycles. The irregular shape of the image boundary is caused by the reflections of the laser sheet from the curved side windows. The images show a very significant intermittency of flow with the high-velocity regions having a spatial dimension of order of 5-10 *mm*. The clearance height at the instance when the PIV is taken is 9.5 mm. Images corresponding to slow cycles have visibly fewer and smaller fraction occupied by the high-velocity regions.

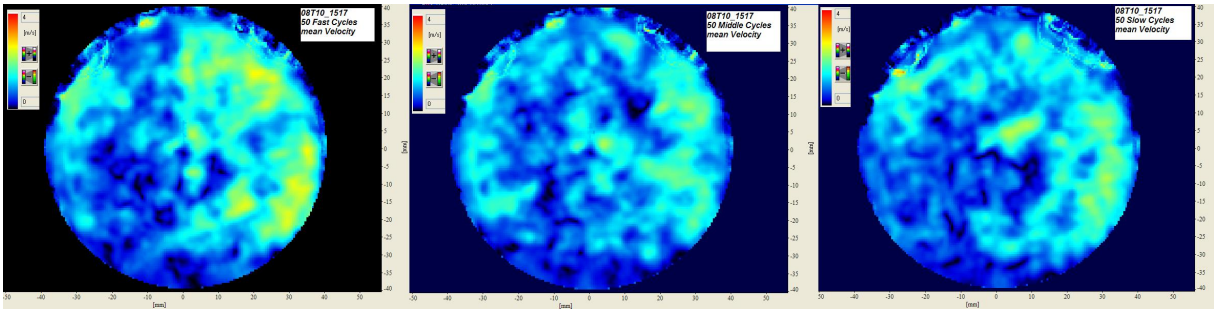

Figure 7. Mean velocitty fields for the fast (left), middle, and slow (right) cycles. The colour bars show the magnitude of the velocity vector.

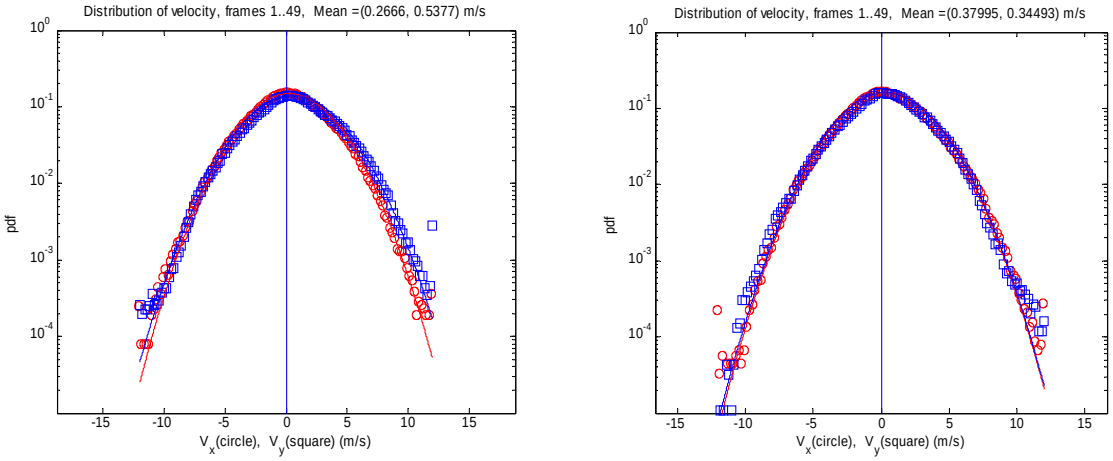

Figure 8. Probability density function for velocity for the fast (left) and slow (right) cycles. Red circles and blue squares denote the u_x and u_y velocity components, respectively.

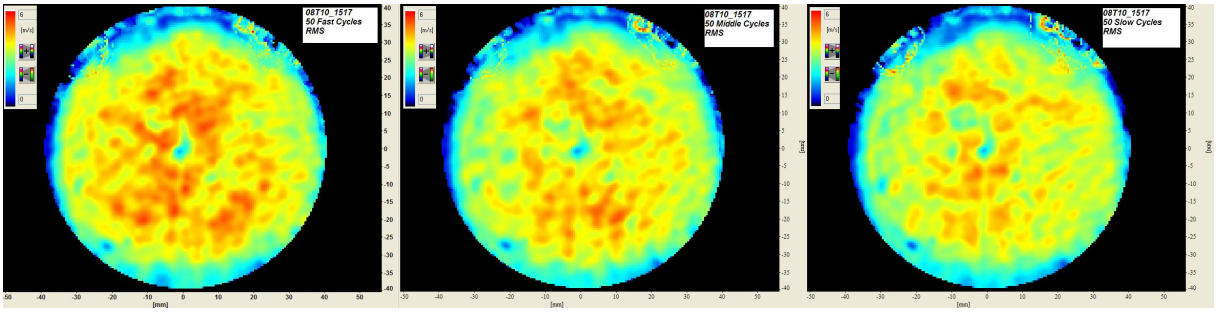

Figure 9. Root-mean-square velocity fields for the fast (lef't), middle, and slow (right) cycles. The colour bars show the magnitude of the rms velocity.

Averaging has been performed separately for fast, middle and slow cycles, over 50 PIV images in each case. Ensemble-averaged velocity fields are shown in Fig. 7; there is a slight asymmetry of the mean velocity field seen on the right and in particular for the fast cycles, however, the inspection of the schlieren images show no discernible flame distortion or faster propagation in this region. Consecutive flame contours remain largely centered on the spark

regardless of whether the cycle is fast or slow. The root-mean-square velocity fields, shown in Fig. 8, reveal rather uniform pattern with a significant decrease towards the walls.

In addition to the average velocity field which show some spatial inhomogeneity and are different for fast and slow cyles, see Fig. 7, the velocity probability density functions (pdf) averaged over the entire flowfield show higher probabilities of large velocity fluctuations, both negative and positive, for slow cycles. Velocity pdf's are shown in Fig. 8 for the fast and slow cycles; the tails of the distribution for large velocity values are such that, to a good accuracy and for any type of cycle $Prob\{(u_x^2+u_y^2)^{1/2}=U\} \sim \exp(-U)$.

Nonetheless, the probability of large velocity fluctuations is low and their contribution to the average root-mean-square (rms) velocity is low. This becomes clear upon comparison of the velocity magnitude rms fields shown in Fig. 9. The fields of the rms velocity are intermittent with the weaker and fewer regions of high rms values corresponding to slow combustion. There is no obvious reason for such intermittency but its presence means correlated motion over finite distances. While the PIV resolution of 0.53 mm in this work does not allow resolution of the entire turbulence spectrum, decomposition of the velocity field into average and fluctuating parts allows one to apply, albeit formally, definitions developed for turbulent flows [15]. In particular, denoting the fluctuating part as u a correlation function f and the integral length scale L corresponding to it may be defined as:

$$f_{xu_x}(r)=\frac{\langle u_x(x,y)u_x(x+r,y)\rangle}{\langle u_x^2(x,y)\rangle} \qquad L_{xu_x}=\int f_{xu_x}(r')dr' \tag{1}$$

For a two-dimensional velocity field there are two longitudinal, f_{xu_x} and f_{yu_y} , and two transversal correlation function, f_{xu_y} and f_{yu_x} , as well as the integral scale derived from those. For homogeneous and isotropic turbulence, the longitudinal length scale is twice larger than the transversal one. Fig. 10 shows the samples of the correlation functions obtained with averaging along the lines of constant x and y. Table 2 lists the values of the scales obtained from these functions. No discernible systematic difference between fast and slow cycles in either correlation length-scales or shapes of the correlation functions can be observed. The transversal scales are only slightly smaller than the longitudinal one.

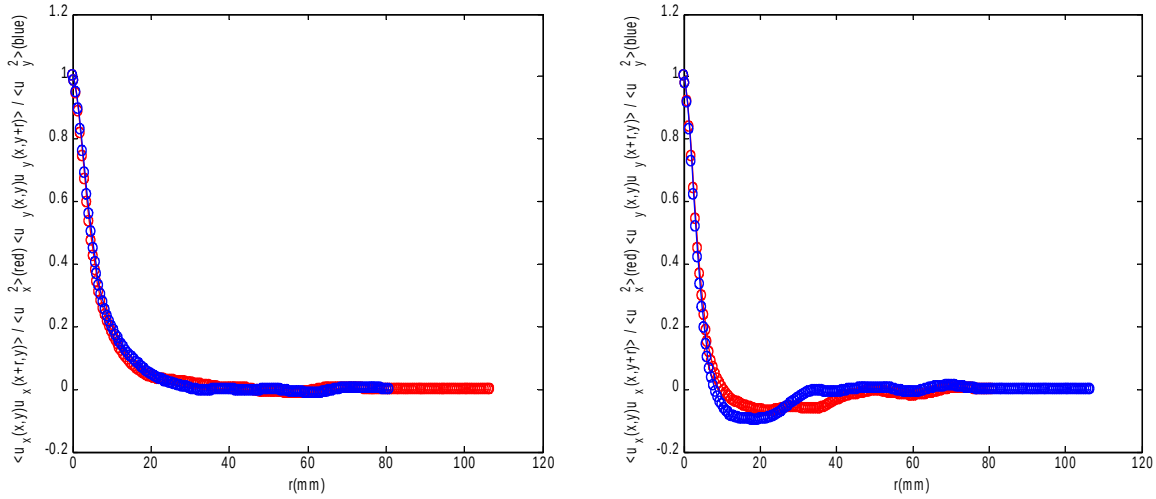

Figure 10. Longitudinal (left) and transversal (right) correlation functions averaged over fifty slow cycles. Left figure: red symbols - f_{xu_x} , blue - f_{yu_y} . Right figure: red symbols - f_{yu_x} , blue - f_{xu_y} .

Table 2. Integral length-scales.

	Longitudinal		Transversal	
	$L_{x\,u_x}$	$L_{y\,u_y}$	$L_{y\,u_x}$	$L_{x\,u_y}$
fast	6.7	7.9	6.0	6.2
middle	6.5	7.8	6.3	5.9
slow	7.0	7.2	6.2	5.7

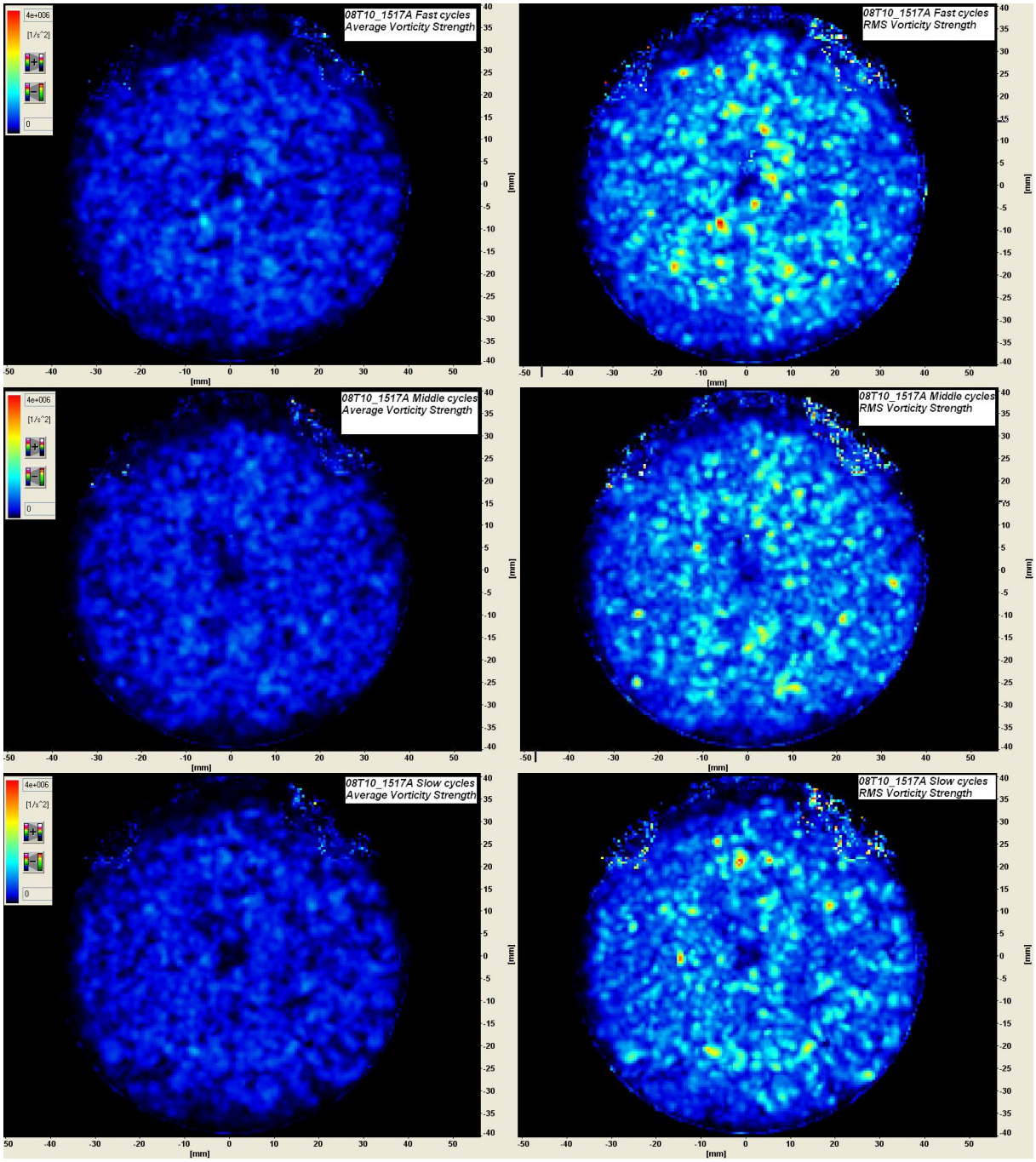

Figure 11. Average (left) and root-mean-square fields of the voricity for the fast (upper two), middle, and slow (lower two) cycles. The colour bars show the magnitude of the vorticity.

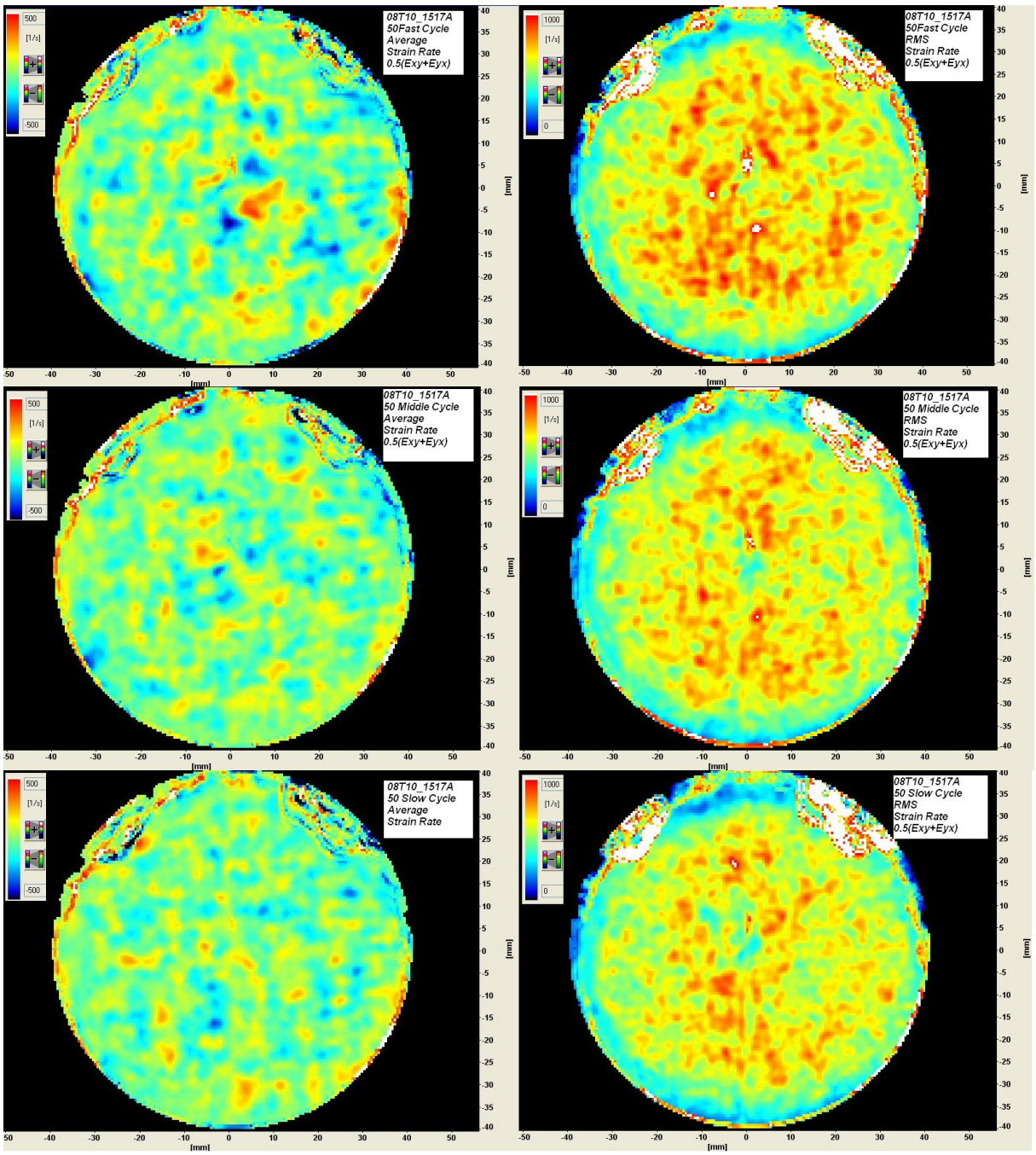

Figure 12. Average (left) and root-mean-square fields of the shear strain rate for the fast (upper two), middle, and slow (lower two) cycles. The colour bars show the magnitude of the strain.

Another two important characteristics of a two-dimensional vector field are its vorticity $\omega = (\partial_x u_y - \partial_y u_x)$ and the shear strain rate $s = \frac{1}{2}(\partial_x u_y + \partial_y u_x)$. Figure 11 show average and rms fields of the vorticity for different types of the cycles, and it can be seen that there is very little variation in the average vorticity between fast and slow cycles, in contrast to the rms values which show clear correlation with the rate of combustion. Faster combustion develop in velocity fields with higher rms vorticity. Similar picture is observed with the shear stress fields shown in Fig. 12. For different types of cycles relatively little difference can be seen between the fields of the average shear strain in contrast with with the rms vlaues. Transition from slow to fast combustion is accompanied with is a marked increase in of the rms shear strain in terms of both the density and amount of the regions with high rms value and

also peak values of $\langle s'^2 \rangle^{1/2}$. (It should be noted that the areas of very large strain rate seen in the upper half near the observation boundary are an artefact caused by the laser sheet reflections from the curved side window of the LUPOE2) .

Discussion

Before turning to the analysis of the observations, it is appropriate to emphasise the strong points and limitations of the deployed experimental arrangements. Use of a large skip-firing ratio allows one to achieve an accurate control of the mixture composition typically unachievable in engine experiments; in particular, dilution of the fresh gas with the residual combustion products has been eliminated. Use of the preheated intake ports ensures nearly perfect homogeneity of the fuel-air mixture. These procedures remove two significant factors often evoked as major reasons of the cyclic variability [4, 5]. And yet, the magnitude of the ccv observed under the present arrangements, that is approximately 20% of the peak pressure scatter, is no different from what is typically measured in a serial engine [6]. The variability of the spark discharge energy and the proportion of energy deposited in the initial kernel [16] are always present in an SI engine, however, as can be seen from Fig. 4, the variability of the initial stages is not related to the burning rate fluctuation in the main phase of combustion. This leaves the variations of the flow field and the air-fuel ratio as the only two probable causes of ccv in the present setup.

In this work, the PIV measurements are taken immediately prior to the spark ignition and an attempt to establish a connection between the velocity statistics at that moment and flame propagation in the subsequent times is therefore tacitly introduces an assumption that the observed flow features persist well into the power stroke. Characteristic time-scale of the intense velocity, or velocity derivatives, patches may be estimated as L/u', where L is a corresponding integral scale and u' is the velocity rms in the patch. From the Table 2 *L~6 mm* while from the Fig. 9 one can infer that the typical u' is about *4 m/sec* hence the lifetime of the observed flow pattern is approximately 1.5 *msec*. At the used engine speed of 1500 rpm this corresponds to 14.5 deg CA, approxiamtely half the total duration of the combustion for the fast cycles, see Fig. 4. Even for the slow cycles, the total duration of the combustion is approximately three times this “Eulerian” integral time scale, therefore, one may reasonaly expect that the large-scale flow pattern observed at the instant of ignition has a large influence throughout the cycle.

Current models of turbulent premixed combustion [1, 17, 18] are largely based on the hypothesis that a) the flame front is a surface and b) the burning rate is deterrmined by the average rate of surface stretch experienced by the flame surface. The rate of stretch is then expressed in terms of the velocity rms and some length (or time) scale. Indeed, our findings, see Fig. 9, do indicate a strong correlation between the rms of the velocity magnitude and the burning rate in individual cycles, nonetheless, data in Fig. 12 show very clearly that it is the root-mean-square rather than the average strain rate of combustion which is an indicator of the burning rate. It is remarkable also that the PIV data reveal the correlation with the burning rate even though the small-scale turbulent motion is not resolved; if this fact is confirmed by the on-going qualitative comparisons it will call for a radical change to the formulation of the models for the rate of combustion in the Large-Eddy Simulations which currently assume that the burning rate is determined by the small-scale “sub-grid” motion.

Acknowledgements

A.M.T.A. El-Dein Hussin gratefully acknowledges the funding from the Egyptian Cultural Bureau. Z.-Y. Ling gratefully acknowledges partial support of his PhD study from China Scholarship Council.

References

[1] J. Heywood, *Internal Combustion Engine Fundamentals*, McGraw Hill, N.Y., 2nd edition, 1988.

[2] K. Liu, C.G.W. Sheppard, A.J. Smallbone, R. Woolley, "The Influence of Simulated Residual and NO Concentrations on Knock Onset for PRFs and Gasolines", *SAE Paper* 2004-01-2998 (2004).

[3] P.J. Roberts, "Fuel and Residual Effects in Spark Ignition and Homogeneous Charge Compression Ignition Engines", PhD thesis, The University of Leeds, 2010.

[4] N. Ozdor, M. Dulger, and E. Sher, "Cyclic variability in spark ignition engines: A literature survey", *SAE Paper* 940987 (1994).

[5] P.G. Aleiferis, Y. Hardalupas, A.M.P.K. Taylor, K. Ishii, and Y. Urata. "Flame chemiluminescence studies of cyclic combustion variations and air-to-fuel ratio of the reacting mixture in a lean-burn stratified-charge spark-ignition engine". *Comb. Flame*, 136:72-90, (2004).

[6] E. Abdi Aghdam, A. A. Burluka, T. Hattrell, K. Liu, C. G. W. Sheppard, J. Neumeister, and N. Crundwell, "Study of Cyclic Variation in an SI Engine Using Quasi-Dimensional Combustion Model", *SAE Paper* 2007-01-0939, (2007).

[7] W.R. Mickelsen and N.E. Ernstein, "Growth rates of turbulent free flames", In IVth Symp. (Int.) on Comb., Baltimore, pp. 325–333, (1953).

[8] K.J. Al-Khishali, P.M. Boston, D. Bradley, M. Lawes, and M.J. Pegg. The influence of fluctuations in turbulence upon fluctuations in turbulent burning velocity. *Proc. Instn. Mech. Engrs*, (C49/83):175–180, (1983).

[9] A.A. Burluka, J.F. Griffiths, K. Liu, and M. Ormsby, "Experimental Studies of the rôle of Chemical Kinetics in Turbulent Flames", *Combustion, Explosion, and Shock Waves*, 45: 383–391 (2009).

[10] H. Shen, P.C. Hinze, and J.B. Heywood, "A study of cycle-to-cycle variations in SI engines using a modified quasi-dimensional model", *SAE Paper* 961187, (1996).

[11] A.N. Lipatnikov and J. Chomiak, "Randomness of flame kernel development in turbulent gas mixture. *SAE Paper*, 982617 (1998).

[12] A.E.S. Eldin Dawood "Combustion and Flow Characteristics in a Disc-shaped Spark Ignition Engine", PhD thesis, The University of Leeds, (2011).

[13] http://www.lavision.de/en/products/davis.php

[14] A. N. Lipatnikov, J. Chomiak, "Turbulent Flame Speed and Thickness: Phenomenology, Evaluation, and Application in Multi-Dimensional Simulations", *Progress in Energy and Comb. Sci.*, 28: 1-74 (2002).

[15] A.S. Monin and A.M. Yaglom, "*Statistical hydromechanics*", "Nauka", Moscow 1965.

[16] R. Maly, "Spark Ignition: Its Physics and Effects on the Internal Combustion Process", in: *Fuel Economy in Road Vehicles Powered By Spark Ignition Engines*, Hilliard, J.C. and Springer, G.S. (Ed.), Plenum, New York, 1984.

[17] J. Ewald, N. Peters, "On unsteady premixed turbulent burning velocity prediction in internal combustion engines", *Proc. Comb. Inst.* 31(2): 3051 - 3058 (2007).

[18] J. A. van Oijen, G.R.A. Groot, R.J.M. Bastiaans and L. P. H. de Goey "A flamelet analysis of the burning velocity of premixed turbulent expanding flames", *Proc. Comb. Inst.* 30: 657 - 664 (2005).